Analytical Methods

Accepted Manuscript

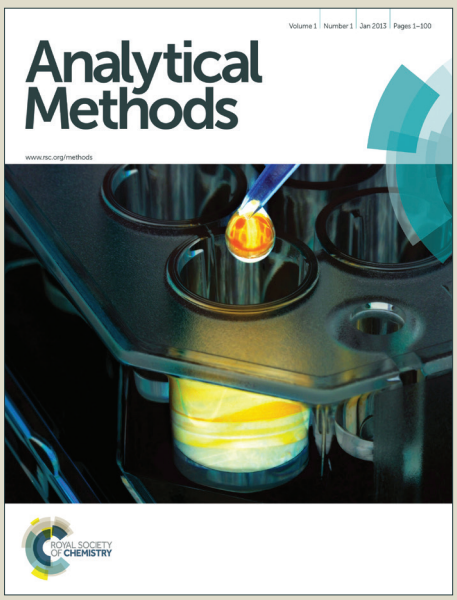

ROYAL SOCIETY OF CHEMISTRY

www.rsc.org/methods

Electrically addressable deposition of diazonium-functionalized antibodies on boron-doped diamond microcells for the detection of Ochratoxin A

Amani Chrouda[a,b], Amel Sbartai[b], François Bessueille[b], Louis Renaud[c], Abderrazak Maaref[a], and Nicole Jaffrezic-Renault*

This work reports the manufacturing procedure for an impedimetric immunosensor for sensitive detection of the mycotoxin, Ochratoxin A (OTA), through electroaddressing of diazonium functionalized antibodies on the working electrode of a planar Boron Doped Diamond (BDD) electrochemical microcell. The immunosensor elaboration and the immunochemical reaction between Ochratoxin A and the surface-bound antibody were monitored using cyclic voltammetry (CV) and electrochemical impedance spectroscopy (EIS). The impedance variation due to the specific antibody–OTA interaction was correlated with the OTA concentration in the samples. The increase in electron-transfer resistance values presents a sigmoidal shape versus log concentration of OTA, with a dynamic range between 7 pg/mL and 25 ng/mL. A limit of detection (LOD) of 7 pg/mL and a IC_{50} of 1.2 ng/mL were obtained. The immunosensor thus fabricated exhibited high sensitivity, good reproducibility, long-term stability, and was used for the detection of OTA in real coffee samples with a good recovery rate. The reported validated manufacturing procedure is compatible with the production of microarrays for multidetection.

.

INTRODUCTION

Ochratoxin A (OTA) is a mycotoxin produced by *Aspergillus* and *Penicillium* species [1, 2]. It has a polyketide derived dihydroisocoumarin moiety linked via a 7-carboxy group to L-β-phenylalanine by an amide bond as shown in Scheme 1. At neutral pH (pH 7.0) in water, OTA is negatively charged. This is due to the ionization of carboxyl (pKa 4.2–4.4) and phenolic moieties (pKa 7.0–7.3) [3]. Therefore both mono- (OTA^-) and dianions of OTA (OTA^{2-}) are present at physiological pH. The presence of ochratoxin A and its diverse forms in nature is due to the ability of OTA-producing filamentous fungi, *Aspergillus ochraceus* and *Penicillium verrucosum*, to grow on a wide range of substrates under varying climatic and storage conditions [4].

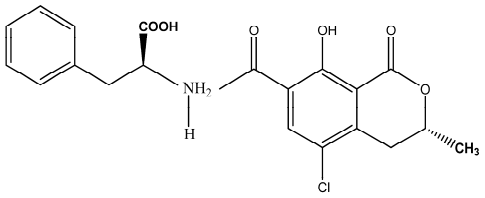

Scheme 1 OTA structure

OTA has been identified as a contaminant in cereals, coffee, cocoa, dried fruits, pork and occasionally in grapes, during storage. It may also be present in the blood and kidneys of animals that have been fed with contaminated foodstuff. Animal studies have indicated that OTA is carcinogenic [5]. Already in 1991 the Joint FAO/WHO Expert Committee on Food Additives (JECFA) evaluated a provisional tolerable weekly intake (PTWI) of 112 ng/kg body weight (b.w.) [6]. In recent years, the European Commission has fixed the maximum concentration of OTA in foodstuffs at 3 µg/kg (7.4 nM) for cereal products, 5 µg/kg (12.4 nM) for roasted coffee

and up to 10 µg/kg (25 nM) for instant coffee. A similar contamination limit has been fixed for dry grapes (10 µg/kg) (EC No. 466/2001, 1881/2006), but a contamination limit of 2 µg/L (5 nM) has been set for wine (EC No. 123/2005). An even lower limit of OTA contamination has been fixed for all baby food (0.5 µg/kg, EC No.466/2001)[7]. Cereals, especially in countries with hot climates, have a strong tendency to be contaminated by OTA. Many works have also reported contamination of grape juices with approximately 7 µg/L OTA[8].

Many immunosensors have found widespread applications in clinical diagnostics, food safety and environmental monitoring [9]. Indeed, from antibodies that show high selectivity and affinity towards mycotoxins like OTA, several immunosensors have emerged for OTA detection including optical waveguide light mode spectroscopy (OWLS) [10], fluorescent biosensor arrays, electrochemicals [11].

Electrochemical Impedance Spectroscopy (EIS) has been successfully used for the direct detection of small molecules but, up to now, only a few papers have reported it for OTA detection[12-16].

A chitosan–polyaniline hybrid conducting biopolymer film was used both for indium–tin-oxide electrode modification and as support for antibody immobilization, a 1 ng/mL detection limit being obtained [13]. Radi et al. reported a label-free impedimetric immunosensor for sensitive detection of ochratoxin with a detection limit of 0.5 ng/mL[14], and an electrochemical immunosensor for ochratoxin A based on the immobilization of antibodies on a diazonium-functionalized gold electrode with a detection limit of 12 ng/mL [17]. A low detection limit (LOD=6.2 pM) has been obtained by immunosensors using antibodies immobilized on carbon nanotubes[18]. Rather high sensitivity (LOD=6 pM) was also obtained with an EIS immunosensor in which the specific antibodies were immobilized on nanostructured zinc oxide deposited onto an ITO covered glass plate [19].

A critical step in the construction of an immunosensor is the antibody immobilization. Adequate antigen–antibody interaction is found when the immobilized antibody is more exposed to the solution (better orientation of antibody for immune reaction) [20]. There is great interest in methods that are able to "address" specific surface regions for functionalization.

Aryl diazonium salts are excellent coupling agents for immobilization of biomolecules (oligonucleotides, enzymes, antibodies) [21–23] as they bind to high-energy surfaces [24-26]. Diazonium chemistry has also been shown to be suitable for the electrically addressable biomolecular functionalization of single-walled carbon nanotubes and vertically aligned carbon fiber electrodes for DNA detection [27].

Corgier et al. introduced the use of diazonium modified antibodies for the direct electrically addressable immobilization of proteins [28]. The main advantages of such an immobilization strategy are ease of preparation, a strong covalent bond between antibody and electrode, and finally the ability to selectively coat and locally control deposition onto electrode platforms.

Boron-doped diamond (BDD) thin films are novel carbon materials and are gaining big interest, especially in the field of biosensors. Recent studies have shown that when diamond surfaces are covalently bonded to biomolecules such as DNA or antibodies, the resulting biologically modified surfaces exhibit extraordinary chemical stability and excellent specificity in biomolecular recognition studies [29-32].

The electrochemical properties of BDD electrodes have also been intensively studied [33–38]. The results showed that BDD electrodes present many outstanding properties, including a wide electrochemical potential window in aqueous electrolytes (about -1.35 V to 2.3 V) [39], excellent mechanical properties, low and stable capacitive background current, high response reproducibility. Therefore, BDD electrodes were found to outperform GC electrodes in terms of stability and sensitivity. In the present work, the surface bio-functionalization was performed by electroaddressing of carboxymethyl aniline (CMA) derivatives of the antibody adducts. CMA was covalently attached to the antibodies by EDC/NHS linkers according to the protocol of R. Polsky et al. [23]. This electroaddressing was performed on the working electrode of a planar Boron Doped Diamond (BDD) electrochemical microcell, this technique being compatible with the production of microarrays for multidetection. Cyclic voltammetry and EIS were used to characterize each immobilization step and the OTA

binding process. In order to determine the OTA concentration, the variation of the impedance due to the antibody–OTA interaction was monitored.

This immunosensor has been successfully tested in a sample of coffee, then combining the significant advantages of the electrochemical detection with a rapid and real time monitoring of the biorecognition event using a specific, stable, and robust biorecognition element.

EXPERIMENTAL

Reagents

Polyclonal antibodies (pAb) (developed in rabbits) against OTA were purchased from Interchim (France). The provided antibody solution contained 5 mg of total protein per mL. It was aliquoted and stored at -20°C until use. Ochratoxin A (OTA) from *Aspergillusochraceus*, received from Sigma-Aldrich, was dissolved in ethanol at 1 mg/mL and stored as aliquots in tightly sealed vials at -20°C. 4-aminophenylacetic acid, *N*-hydroxysuccinimide (NHS), 1-ethyl-3-(3-dimethylaminopropyl)-carbodiimide hydrochloride (EDC), potassium ferricyanide ($K_3[Fe(CN)_6]$), potassium ferrocyanide ($K_4[Fe(CN)_6]$), sodium chloride (NaCl),potassium chloride (KCl),dimethyl sulfoxide (DMSO), sodium phosphate dibasic (Na_2HPO_4), potassium phosphate monobasic (KH_2PO_4), sulfuric acid (H_2SO_4) (98%), and ethanol (98%) were all supplied by Sigma–Aldrich (France). Milli-Q ultrapure water (resistivity = 18.2 MΩ.cm) was used in all experiments. Phosphate buffer saline (PBS) with pH 7.0 containing 140 mM NaCl, 2.7 mM KCl, 0.1 mM Na_2HPO_4 and 1.8 mM KH_2PO_4 was used. A 5 mM potassium ferricyanide/ferrocyanide solution prepared in PBS was used in EIS and CV experiments.

Instrumentation

Preparation of the BDD electrochemical cell

Electrochemical microcells were made from a film of 300 nm of boron-doped microcrystalline diamond (BDD) deposited on an insulated silicon wafer 101.6 mm in diameter provided by the NEOCOAT company (La Chaux-de-Fonds, Switzerland). 300 nm thick polycrystalline boron-doped diamond with a boron concentration higher than 7000-8000 ppm was grown by MPECVD on silicon coated with an insulating layer of silicon oxide, and silicon nitride ($Si/SiO_2/Si_3N_4$), 0.5 µm thick. The three electrodes, the working electrode (1 mm diameter), counter electrode and pseudo-reference electrode, were cut out of the BDD wafer by micromachining [39].

Achieving direct machining has a significant advantage over conventional photolithography, because only one step is needed to make all electrochemical microcells, the process is fast and without chemical reagent. Another characteristic of direct machining is that the computer controls the path of the laser beam relative to the work-piece. This helps one to obtain quickly and accurately repeatable structures and whether changes are needed, the laser control software can quickly be modified accordingly. The micromachining was performed by the MANUTECH USD (Saint-Etienne, France) Company using a femtosecond laser (5 kHz, 2.5 W, 800 nm, 150 fs); a scanner head; a set of XYZ moving plates. The parameters used during processing were: power 150 mW; optic scanner 80 mm and speed 10-20 mm/s. The micro-cell resulting from laser machining is shown in Photo 1. The working electrode is in the centre, around it is the "reference", and the counter electrode is on the edge. Instead of the conventional saturated calomel electrode (SCE), the device used a pseudo-reference made of BDD [39].

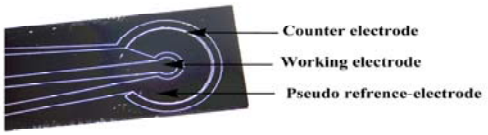

Photo 1 BDD microcell; the working electrode is in the center, around it is the pseudo-reference and the counter electrode is on the edge.

Apparatus for electrochemical measurements

The PalmSens sensor PC interface (Eindhoven, The Netherlands) was used to perform cyclic voltammetry. The interface was connected to a PC computer. A Voltalab 40 impedance analyzer (Radiometer Analytical) was used to perform the impedance measurements, in the frequency range 100 mHz–100 kHz, using a modulation voltage of 10 mV. Zplot/Zview modeling software (Scriber and Associates, Charlottesville, VA) was used to fit the faradaic impedance spectra.

Experiments were carried out with a 5 µL flow cell made of PEEK provided by BVT Technology (Czech Republic). Instead of the conventional saturated calomel electrode (SCE), the device used a pseudo-reference made of BDD. An O-ring seal defined the measuring volume, and the electrical contacts were obtained by pressure on the front side of the BDD electrodes (Photo 2).

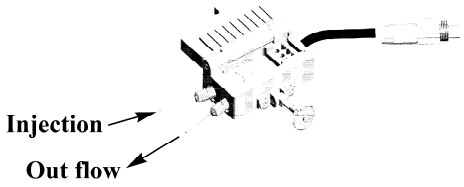

Photo 2 Flow cell for integration of a BDD microcell

Procedure for immunosensor elaboration

Immunoglobulin modification

First, 10 mg of 4-carboxymethylaniline were activated in the presence of 20.6 mg of EDC, and 11.5 mg of NHS in 1ml of DMSO for 30 min under stirring. Then 20µl of the activated CMA were added to 500µl of a 5 mg/mL antibody solution in 0.1M carbonate buffer, pH = 11. This coupling solution was left to react for 2 hrs under stirring at room temperature and then CMA modified antibody was concentrated by centrifugation. The obtained retentate was covered in 100 µL of distilled water and stored at +4 °C [28].

Diazotation and electrodeposition of 4 –carboxy-methylaniline modified antibody

The BDD microcells were cleaned and activated by 10 mL of Piranha solution (H_2SO_4 (95−97%)/H_2O_2 (30%), [V/V = 7:3]) for 5 min. BDD microcells were then rinsed with distilled water, dried with nitrogen. After cleaning, the CMA modified antibody adducts were diazotated in an aqueous solution by using 20mM HCl, 20mM $NaNO_2$ for 10 min under stirring at 0°C. Electro-addressing was achieved by directly depositing on the BDD working electrode surface, so a potential was applied from 0 to -1000 mV at a scan rate of 100 mV/s.

OTA detection by EIS measurements

After electrodeposition of the antibody on the surface of BDD micocells, the electrode was rinsed with distilled water. After that the modified electrode was incubated in different concentrations of OTA (7 pg/mL – 25 ng/mL) for 30 min. These measurements were carried out using a ferro/ferricyanide couple (3 mM) in PBS buffer with pH 7.4. The frequency range was 100 mHz to 100 kHz, using a modulation voltage of 25 mV. The potential applied to the BDD electrode was fixed at −300 mV versus a pseudo-reference electrode.

Morphological study of BDD surfaces: AFM measurements

The AFM measurements were carried out using an Agilent 5500 AFM (Agilent Technologies, Palo Alto, CA, USA). Silicon tips with a nominal spring constant of 20 Nm^{-1} were used in tapping mode at a frequency of ~300 kHz. The scanned area was always 25 µm×25 µm.

RESULTS AND DISCUSSION

Diazonium-modified antibody deposition on BDD surface

The procedure for the preparation of the diazonium-modified antibody and subsequent electrical immobilization is presented in Scheme 2 .A carboxyl diazonium molecule is covalently attached to free primary amine groups on an anti-OTA antibody by EDC/NHS cross-linking in 0.1M carbonate buffer, pH = 11.

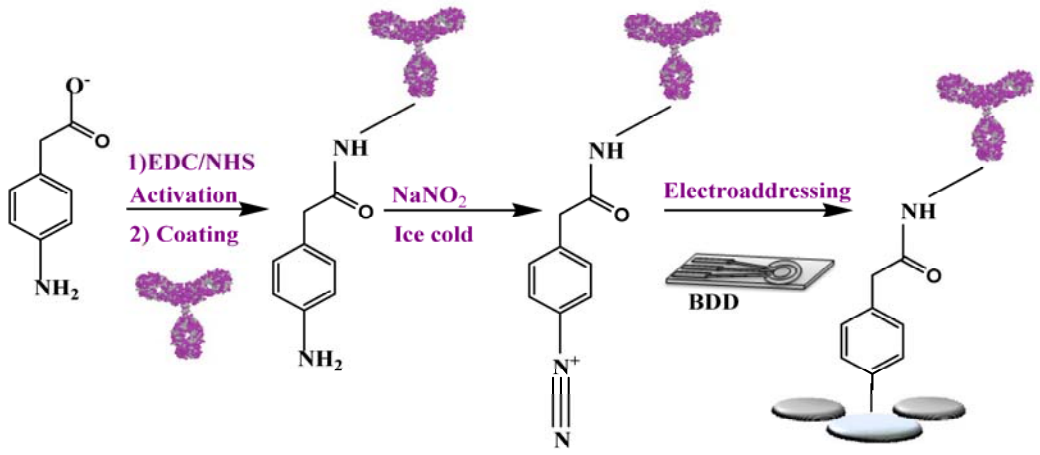

Scheme 2 Strategy for direct electro-addressing of modified antibody onto BDD microcell surface

Electrochemical monitoring

The initial cycle in Fig. 1 shows a broad and irreversible cathodic wave with a peak potential at about −1 V that indicates diazoted CMA-modified antibody attachment onto the BDD surface by diazonium salt reduction. This radical was previously shown to attack the surface and to form a covalent bond between the aryl group and the surface carbon atoms of the BDD microcell [40].The reduction peak disappears only from the third cycle, then 3 cycles were applied**.**

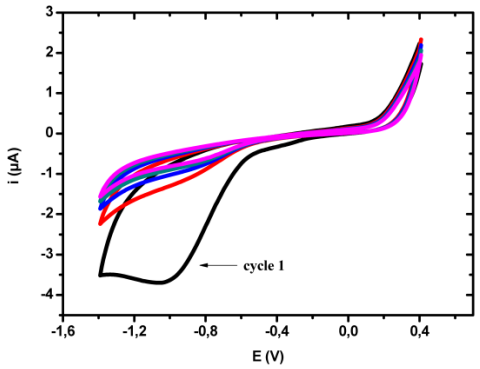

Fig.1 Cyclic voltammograms of 4-carboxymethylaniline modified antibody (5 mM), potential scanned from 400 to -1400 mV on BDD microcell electrode. Five cycles performed scan rate of 100 mV/s.

Electrochemical characterization

- *Cyclic voltammetry*

Cyclic voltammetry was used to characterize each immobilization step for the immunosensor elaboration, using $K_3(Fe(CN)_6)/K_4(Fe(CN)_6)$ [5 mM] in PBS buffer at pH 7.4. An important decrease of the maximum peak intensity of the CV cycles was observed (Fig. 2) when compared to the bare BDD microcell (curve a). This indicates that the CMA modified antibody layer has a blocking effect on the electroactive surface.

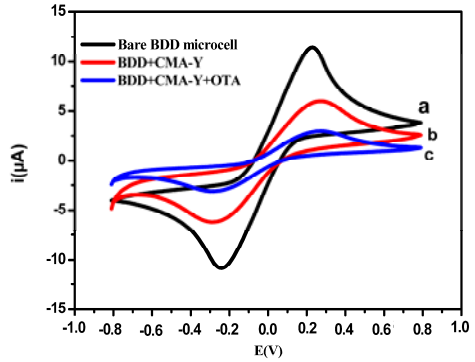

Fig. 2 Cyclic voltammograms scan for: (a) bare (b) CMA-Ab immobilized onto the BDD microcell (c) after formation of immunochemical complex at the surface of the CMA-Ab / BDD modified electrode exposed to 0.1 ng.mL^{-1} OTA solution for 30 min

- ***Electrochemical impedance spectroscopy***

The successful immobilization of each functionalized layer was confirmed through EIS measurements. Fig. 3A shows the Nyquist plots of impedance spectra after each surface modification step. On the basis of the charge transfer kinetics of the $[Fe(CN)_6]^{3-/4-}$ redox probe, the faradic impedance spectra were modeled using the equivalent circuit (Fig. 3A). The circuit includes the series resistance (R_s), Q_{CPE1} reflecting the non-homogeneity of negative and positive charges at the Boron Doped Diamond electrode interface; the charge transfer resistance R_{ct1} which reflects the direct charge transfer to and from the BDD surface (this corresponds to the first small semicircle of the Nyquist plot), the second R_{ct2} describes the electron transfer at the electrolyte/immobilized substances, including CMA-Y (this correspond to the second semicircle of the Nyquist plot) and, finally, the second Q_{CPE2} which reflects the non-homogeniety of the charges at the biolayer interface in the presence of the OTA molecules.

Table 1 shows the simulated parameters from the impedance data obtained for each step of the immunosensor elaboration. The R_{ct2} was found to be the most sensitive to the changes in each steps of modified electrode, thus, selected as the relevant parameter to monitor the sensitivity and selectivity of the developed immunosensor.

The Nyquist plot for a bare BDD microcell presents a very small semi-circle appears at high frequencies, suggesting a very low electron transfer resistance to the redox probe dissolved in the electrolyte solution (curve a) and a straight Warburg line with a slope near unity in the low frequency domain characteristic of a semi-infinite diffusion phenomenon. The charge-transfer calculated from the semicircle diameter is R_{ct1}= 18 Ω. A big advantage of the BDD electrode is also due to the facility of quickly changing its surface properties.

In the comparison of the charge transfer resistance and capacity of double layer listed in Table 1, R_{ct1}, Q_{CPE1} kept nearly constant even with different biomolecule modifications on BDD microcell.

Nyquist plots (Fig. 3B) of modified microcell (BDD-CMA-Y; curve b) exhibits a significant increase of

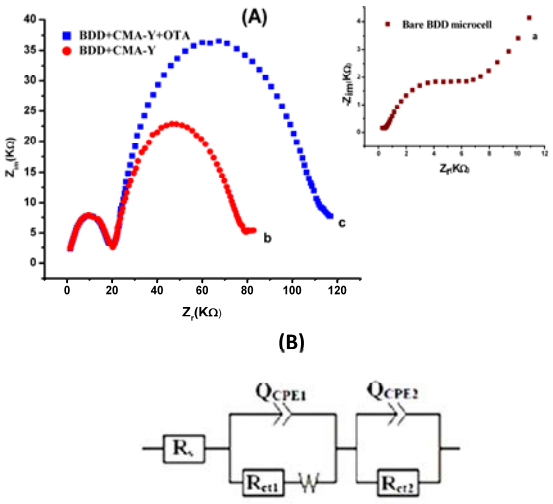

Fig. 3 A Nyquist plot of EIS measurements (a) Bare BDD microcell (b) CMA-Y modified BDD microcell (c) CMA-Y+ 0.1 ng/mL OTA and **B** an electrical equivalent circuit for both a bare and a modified electrode

charge-transfer resistance (R_{ct2} = 87KΩ) value obtained by fitting with an equivalent circuit (Fig.3B). This result clearly demonstrates denser structure of the modified layers which decrease the electron transfer rate. This result is in agreement with the study in cyclic voltammetry.

Using equation 1, the coverage for CMA-Y modified BBD microcell was estimated to be 80%.

$$\mathbf{1 - \theta = \frac{R_{ct1}}{R_{ct2}}} \quad (1)$$

Where ɵ is the apparent electrode coverage, $R_{ct1}$and R_{ct2} corresponds to charge-transfer resistance value of initial BDD electrode and CMA-Y modified BBD electrode. The increase of charge-transfer resistance (R_{ct2}) is proportional to electrode coverage due to the immobilization of biolayer.

After 30 minutes incubation of the BDD-modified electrode in the solution of 0.1 ng/mL OTA at 4°C, a significant increase in the blocking effect was observed (R_{ct2} increased curve c). At hight frequency, the first semi-circular part of the Nyquist diagram was not affected after OTA incubation, showing that only the electrolyte/film interface is modified during this OTA incubation. These results demonstrate that the characteristic signal derived from the antibody–antigen reaction and the electrode tailored in this fashion is suitable for an electrochemical immunoassay format.

Characterization of surface morphology

The electrografted film was well located on the working electrode (data not shown), then masking the microcrystalline structure of BDD (Figure 4A), the mean diameter of microcrystallites being 200 nm (surface rms 46 nm). The AFM images show that the film of the CMA-modified antibodies was homogeneous and dense, showing a more flat surface (rms 38 nm) (cf Figure 4B). The mean thickness of the film was determined to be 180 nm, corresponding to a total coverage of the BDD microcrystallites.

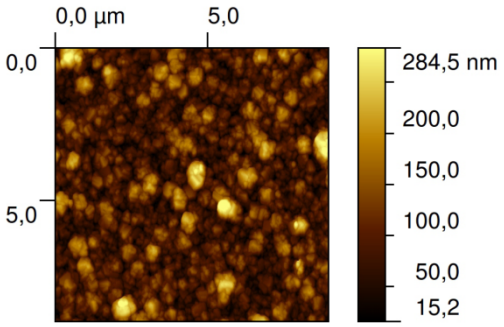

Fig. 4A AFM image of bare BBD microcell

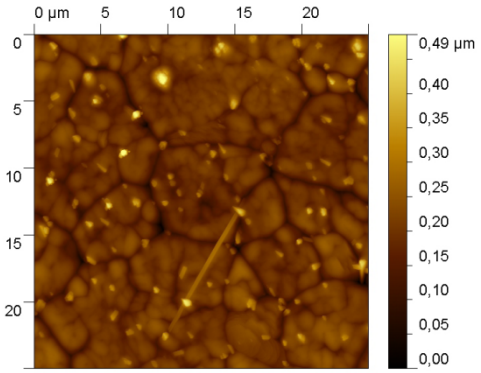

Fig. 4 AFM image of CMA- modified antibodies electrodeposited on BBD microcell

Table 1 Values of the equivalent circuit parameters of the fitting curves for the various steps of the immunosensor elaboration and the immunochemical reaction between antibody and ochratoxin A.

Electrodes	$R_s(\Omega)$	$R_{ct1}(\Omega)$	$Q_{CPE1}(F)/n$	$R_{ct2}(\Omega)$	$Q_{CPE2}(F)/n$
Bare BDD	**5.3**	**18.6**	**$2.4x10^{-8}$**		
BDD/CMA-Y	**5.5**	**18.9**	**$2.2x10^{-8}$**	**87**	**$4.5x10^{-7}$**
BDD/CMA-Y/OTA	**5.9**	**19.3**	**$2.6x10^{-8}$**	**123**	**$5.2x10^{-7}$**

Electrochemical detection of ochratoxin A using EIS immunosensor

To evaluate the immunochemical reaction between Ab and OTA, we exposed the Ab modified BDD microcell to various concentrations of OTA. It was found that the diameter of the Nyquist circle increased with the adding of OTA, indicating that the increase in the charge transfer resistance (Fig.5). Using Zplot/Zview software, the value of ΔR_{CT} was calculated for each OTA concentration by fitting the experimental data. The increase in R_{ct} is directly proportional to the log of OTA concentration, explained by the fact that the OTA binding to surface-bound Ab offers additional negative charges. The OTA molecule has a carboxyl and a phenolic functional group which give the OTA molecule two anionic forms: a monoanion (OTA^-) and a dianion (OTA^{2-}) both present at pH 7.0 [16]. The existence of the two anionic states explains the blocking

Table 2 A comparisons of the analytical characteristics of the immunosensor developed in this work with relevant immunosensors for Ochratoxin A detection from the literature concentrations of OTA (7pg/mL-25 ng/mL).

Type of transducer	Limit of detection ng/mL	Dynamic Range ng/mL	Materials electrode	References
Impedance	3	0-10	TIO_2	[12]
	1	1-10	ITO	[13]
	0.5	1-20	Gold	[14]
	0.01	0.01-5	Gold	[16]
	12	0-60	SPGE	[17]
	7.10^{-3}	7.10^{-3}-25	BDD	This work

effect of surface-bound OTA molecules for electron transfer. This could also be partly due to conformational changes in antibody molecule after the formation of complexes with antigen [14].

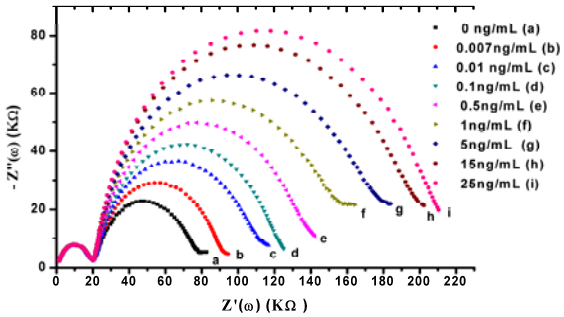

Fig. 5 Nyquist plots after immunosensor incubation with different OTA concentrations: (a) 0 ng/mL; (b) 0.007 ng/mL; (c) 0.01 ng/mL; (d) 0.1 ng/mL; (e) 0.5 ng/mL; (f) 1 ng/mL; (g) 5 ng/mL ; (h) 15 ng/mL ; 25 ng/mL in (5 mM K3[Fe(CN)6]/K4[Fe(CN)6], polarization potential −300 mV. , frequency 100 mHz to 100 kHz).

Analytical characteristics of the immunosensor

Calibration curve

The calibration curve is presented in Fig. 6 as the variation of the charge transfer resistance $\Delta R_{ct} = R_{ct(Ab-Ag)} - R_{ct(Ab)}$ versus log of OTA concentration. It was found that saturation of the electrode occurred at concentration values higher than 25 ng/mL OTA. This phenomenon is caused by the binding of all the available active sites of the antibodies on the electrode surface, the dynamic impedimetric immunosensor ranging from 7pg/mL to 25 ng/mL. After performing the measurements, response curves are fitted to the following four parameter equation :

$$Y = \left\{\frac{A-B}{1-\left(x/C\right)^{D}}\right\} + B \qquad (2)$$

Where A is the absolute maximal signal (infinite analyte concentration), B is the absolute minimum signal (zero analyte concentration), C is the concentration producing 50 % of the maximal signal change (IC50), and D is the slope at the inflection point of the sigmoid curve, fitted by the sigmoidal logistic four parameter-equations.

The obtained IC50 is in the lower range of those in some The LOD (7 pg/mL) corresponding to less than 1 % of binding, and IC50 (0.75 ng/mL) corresponding to 50 % of binding [41] were calculated from the calibration curve (Fig. 6), previous studies, between 0.37 to 30 ng/mL [42-45]. This low IC50 value facilitates a quite sensitive assay.

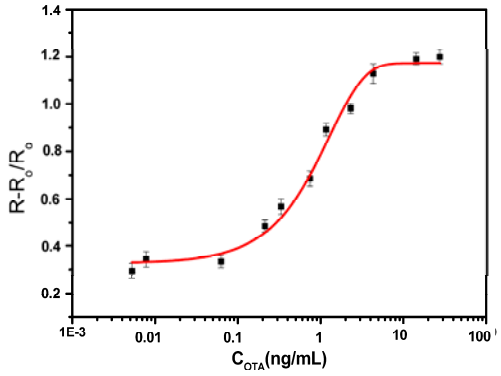

Fig.6 Response curve of the impedimetric immunosensor, using the covalent immobilization technique, for the Ochratoxin A detection

The found LOD is one of the lowest results reported in the EIS[12-14, 16, 17], SPR [46] or QCM [47]detection of OTA.

The new electrochemical approach used in this paper shows a very sensitive response to OTA compared to the previous impedimetric immunosensor based on other types of electrode materials (TiO_2, ITO, gold, SPGE) (Table2).

Stability and reproducibility of immunosensor

A long-time stability of the immunosensor was studied on a 14 day period. After keeping it in refrigerator (4 °C) for 2 weeks, the immunosensor was used to detect an OTA concentration of 5 ng/mL. The relative variation of charge transfer resistance was found to be lower of 5% than that of the newly prepared immunosensor, demonstrating that the immunosensor presents a good stability.

The reproducibility of the immunosensor was studied by preparing seven different immunosensors. The resulting relative standard deviation (RSD) was found to be 3.7%. The experimental results indicate a good reproducibility of the fabrication protocol.

Specificity

In order to confirm that the observed impedance changes were indeed based on the specific interaction between the CMA-Ab immobilized on the electrode surface and OTA

A first one was prepared with the antibody anti OTA (CMA-Y), a second sensor was fabricated utilizing a non-specific antibody (anti-*staphylococcus aureus* antibody) in place of the specific OTA antibody, and the third sensor is modified without any antibody. The histogram presented in Fig. 7 shows the sensitivity of the response of sensors.

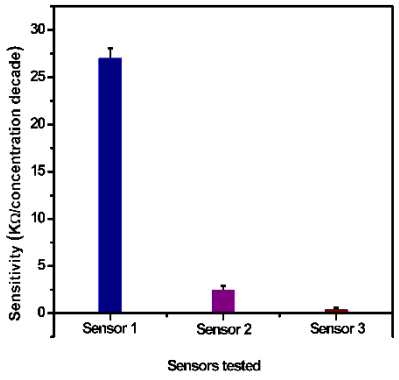

Fig. 7 Sensitivities to OTA for three different sensors: Sensor 1 modified with anti-OTA antibody; Sensor 2 modified with anti-staphylococcus; Sensor 3 without any antibody.

This representation clearly confirms that the observed sensitivity is totally correlated to the specific antibody-OTA interactions and not caused by non-specific adsorption; different sensors were elaborated in the same conditions.

OTA detection in coffee beans

In order to check the performance of the developed immunosensor for the detection of OTA in coffee beans, OTA was first extracted by mixing 25 g of ground coffee beans (commercial Arabica coffee) and 500 mL of methanol/aqueous sodium hydrogen carbonate (50:50).

The suspension was shaken for 3 min. The mixture was filtered through Whatman no. 4 filter paper, and then 4 mL of the filtrate was diluted to 100 mL [43].

The concentration was calculated from the calibration curve and the concentration of OTA found after final dilution was 0.15 ng/mL, which corresponds to 80 µg/kg of coffee beans. This concentration value was also found using HPLC/MS/MS. In Ref [44], the concentration of OTA determined in roasted coffee beans was equal to $5x10^{-7}$M, corresponding to 200 µg/kg, in the same order of magnitude as our results.

CONCLUSION

In this paper, a sensitive label-free electrochemical immunosensor for sensitive detection of OTA has been developed on BDD microcells. We show that the direct electrically addressable deposition of diazonium-electrochemical immunosensing formats. The response of the immunosensor by electrochemical impedance spectroscopy for the detection of OTA yields an analytically attractive performance. The immunosensor was finally successfully applied to the determination of OTA in a real sample (coffee).

Our results show that these novel BDD microcells present the advantage of allowing a highly stable, sensitive, selective and specific detection. Multiplexed multisensors will be designed using the laser micromachining of BDD film and electro-addressing of CMA-Abs will be applied for the elaboration of a multisensing immunoplatform.

ACKNOWLEDGEMENTS

The authors would like to thank CAMPUS-FRANCE for financial support through PHC Maghreb no. 12 MAG 088. A. Chrouda thanks the Tunisian government for her Mobility Grant.

NOTES AND REFERENCES

[a]Laboratory of Interfaces and Advanced Materials, University of Monastir, Avenue of Environment, 5019 Monastir, Tunisia
[b]University of Lyon, Institute of Analytical Sciences, UMR CNRS 5280, 5 La Doua street, 69100 Villeurbanne, France
[c]University of Lyon, Institute of Nanotechnology of Lyon, UMR CNRS 5270, 43 Boulevard 11 November 1918, 69622 Villeurbanne Cedex, France

*Corresponding author: Phone: +33437423558; e-mail: nicole.jaffrezic@univ-lyon1.fr

1 S. C. B. Oliveira, V. C. Diculescu, G. Palleschi, D. Compagnone and A. M. Oliveira-Brett, *Anal. Chim. Acta*, 2007, **588,** 283-291.

2 P. Zollner and B. Mayer-Helm, *J. Chromatogr. A*, 2006, **1136,** 123–169

3 H. Valenta, J. *Chromatogr. A*, (1998), **815,** 75-92.

4 B. Prieto-Simon, M. Campos, J.-L. Marty and T. Noguer, *Biosens. Bioelectron*, 2008, **23,** 995-1002.

5 M.A. Alonso-Lomillo, C. Yardimci, O. Dominguez-Rened and M.J. Arcos-Martinez, *Anal Chim Acta*, 2009, **633,** 51-56.

6 A. El Khoury and A. Atoui, *Toxins*, 2010, **2**, 461-493.

7 D.P Nikolelis (Eds) Portable Chemical Sensors: Weapons Against Bioterrorism, Springer Series: NATO Science for Peace and Security Series A: *Chemistry and Biology*, 2012.

8 H. Bejaoui, F. Mathieu, P. Taillandier and A. Lebrihi, *J. Appl. Microbiol*, 2004, **97**, 1038–1044.

9 A. Ramanavicius, A. Finkelsteeinas, H. Cesiulis and A. Ramanaviciene, *Bioelectrochemistry*, 2010, **79**, 11-16.

10 W-C. Chen, T-C.Wen, C-C. Hu, A. Gopalan, *Electrochim. Acta*., 2002, **47**, 1305 -1315.

11 S. H. Alarcon, G. Palleschi, D. Compagnone, M. Pascale, A. Visconti and I. Barna-Vetro, *Talanta*, 69, 2006, 1031–1037.

12 R. Khan and M. Dhayal, *Electrochem. Commun*., 2008, **10**, 492-495

13 R. Khan and M. Dhayal, *Biosens Bioelectron*., 2009, **24**, 1700-1705.

14 A.E. Radi, X. Munoz-Berbel, V.Lates and J.L. Marty, *Biosens Bioelectron*., 2009,**24**, 1888-1892.

15 Kaushik, P. R. Solanki, A. A. Ansari and S. Ahmad, B. D. Malhotra, *Electrochem. Commun*., 2008, **10**, *1364*-1368.

16 L.G. Zamfir, I. Geana, S. Bourigua, L. Rotariu, C. Bala, A. Errachid and N. Jaffrezic-Renault, *Sensor Actuat B-Chem*., 2011, **159**, 178–184

17 A-E. Radi, X. Munoz-Berbel, M. Cortina-Puigc and J-L. Marty, *Electrochim Acta*., 2009, **54**, 2180–2184

18 Kaushik, P. R. Solanki, M. K. Pandey, K. Kaneto and S. Ahmad, B. D. Malhotra, *Thin Solid Films*, 2010, **519**, 1160-1166..

19 Ansari, A. Kaushik, P. R. Solanki and B. D. Malhotra, *Bioelectrochemistry*, 2010, **77**, 75-81.

20 Margni,Inmunologiae Inmunoquimica. Fundamentos, 5th ed., Panamericana, Buenos Aires, 1996.

21 A. Shabani, A.W.H. Mak, I. Gerges, L.A. Cuccia and M.F. Lawrence, *Talanta,* 2006, **70**, 615–623.

22 G.Z. Liu and J.J. Gooding, *Langmuir*, 2006, **22**,7421-7430.

23 R. Polsky, J.C. Harper, D.R. Wheeler, S.M. Dirk, D.C. Arango, S.M. Brozik, *Biosens. Bioelectron*., 2008, **23**,757-764.

24 D.E. Jiang, B.G. Sumpter and S. Dai, *J. Am. Chem. Soc*., 2006, **128**, 6030-6031.

25 D.E. Jiang, B.G. Sumpter and S. Dai, *J.Phys. Chem. B*., 2006, **110**, 23628-23632.

26 N. Shao, S. Dai, D.E. Jiang, in: M.M. Chehimi (Ed.), Aryl Diazonium Salts: New Coupling Agents in Polymer and Surface Science., 2012, p. 1–35.

27 C.S. Lee, S.E. Baker, M.S. Marcus, W.S.Yang, M.A. Eriksson and R.J. Hamers, *NanoLett*, 2004, **4**,1713-1716.

28 B. P.Corgier, C. A.Marquette and L. J. Blum, *J. Am. Chem. Soc*, 2005, **127,** 18328-18332.

29 W. S.Yang, J. E.Butler, J. N., Jr. Russell and R. J. Hamers, *Langmuir*, 2004, **20**,6778- 6784.

30 W. S.Yang, O. Auciello, J. E. Butler, W. Cai, J. A. Carlisle, J. E. Gerbi, D. M. Gruen, T. Knickerbocker, T. L. Lasseter, J. N., Jr. Russell, L. M. Smith, R. J. Hamers, *Nat. Mater*., 2002, **1**,253-257.

31 T. Knickerbocker, T. Strother, M. P. Schwartz, J. N., Jr. Russell, J. E. Butler, L. M. Smith and R. J. Hamers, *Langmuir*, 2003, **19**,1938-1942.

32 M. C. Lu, T. Knickerbocker, W. Cai, W. S. Yang, R. J. Hamers and L. M. Smith, *Biopolymers*, 2004, **73**,606-613.

33 F. Bouamrane, A. Tadjeddine, J. E. Butler, R. Tenne, and C. Lévy-Clément, *J Electroanal Chem*., 1996, **405**,95-99.

34 A. E. Fischer, Y. Show and G. M. Swain, *Anal Chem*., 2004,**76**, 2553-2560.

35 R. G. Compton, J. S. Foord and F. Marken, *Electroanal*., 2003, **15**,1349-1363.

36 M. C. Granger, M. Witek, J. Xu et al., *Anal Chem*., 2000, **72**, 3793-3804.

37 T. A. Ivandini, R. Sato, Y. Makide, A. Fujishima, and Y. Einaga, *Diam. Relat. Mater*., 2004, **13**,2003-2008.

38 E. A.; Swain, G. M. *Anal. Chim. Acta*., 2006, **575**,180-189.

39 A. Sbartai, P. Namour, A. Errachid, J. Krejči, R.Šejnohová, L. Renaud, M- L. Hamlaoui, A-S. Loir, F. Garrelie, C. Donnet, H.Soder, E. Audouard, J. Granier and N. Jaffrezic-Renault, *Anal. Chem*., 2012, **84**,4805-4811.

40 Z. Salmi, A. Lamouri , P. Decorse , M. Jouini , A. Boussadi , J. Achard , A. Gicquel , S. Mahouche-Chergui , B. Carbonnier and M. M. Chehimi, *Diam. Relat. Mater*., 2013, **40**,60-68.

41 B. Prieto-Simon, M. Campas, J.L Marty and T. Noguer, *Biosensors and Bioelectron*., 2008, **23**, 995–1002.

42 W.B. Shim, , A.Y. Kolosova, , Y.J. Kim, Z.Y.Yang, S.J.Park, S.A. Eremin, I.S. Lee, and D.H. Chung, *Intl. Food Science and Technology*, 2004, **39**, 829–837.

43 J.H. Park, D.H. Chung, and I.S. Lee, *Life Science.* 2006 , **16**, 1006–1013.

44 F.Zezza, F. Longobardi, M.Pascale, S.A.Eremin and A.Visconti, *Analy.Bioanaly. Chem*.. 2009, **395,**1317–1323.

45 J.A.Cruz-Aguado and G . Penner, *Analy. Chem.* 2008, 80, 8853–8855.

46 J. Yuan, D.W. Deng, D.R. Lauren, M.I. Aguilar and Y.Q. Wu, *Anal Chim Acta*., 2009 **656**,63-71.

47 J.C. Vidal, P. Duato, L. Bonel and J.R. Castillo, *Anal Bioanal Chem*., 2009, **394**,575-578.

48 N.E. Ahmed, M. M. Farag, K. M. Soliman, A. K. M. Abdel-Samed and KH. M. Naguib, *J. Agric. Food Chem*., 2007, **55**, 9576-9580

49 M.A. Alonso-Lomillo, O.Domínguez-Renedoa, L. Ferreira-Goncalves and M. J. Arcos-Martínez, *Biosens Bioelectron*., 2010, **25**,1333-1337.